Monte Carlo (Hybrid) Suprathermal Electron Transport

R. J. Mason
Laser Division, Los Alamos Scientific Laboratory, Los Alamos, New Mexico 87545
(Received 16 July 1979)

A one-dimensional hybrid model for electron transport in laser targets is introduced, in which the suprathermal electrons are collisional particle-in-cell particles, the thermal electrons are a donor-cell fluid, and the electric field is calculated by artificially dilating the plasma period. The scheme shows that resistive electric fields are too transient and that a calculated ion-acoustic level is too low to explain experimentally observed reduced transport, that can, however, arise as convective inhibition enhanced by troughs in the target density profile.

The energy absorbed into laser targets is distributed by suprathermal electrons throughout a background of cooler thermal electrons, ultimately determining the target hydrodynamics.[1] The physics of this transport is in controversy, with experiments indicating inhibition that is unexplained by theory.[2,3] Various transport models are available,[4-8] but a comprehensive algorithm has been lacking, since it must track the distribution of suprathermals to model preheat[1,7] in the collisional target interior, while confining both hot and cold components with a self-consistent electric field in the collisionless target corona. Also, it must manage the coupling and the relative convection of the two components. This Letter introduces a new Monte Carlo hybrid scheme for treatment of the full one-dimensional transport problem. With it, for the first time, we demonstrate (a) thermal inhibition from convection and thermoelectric fields in response to collisionless suprathermal currents, and (b) inhibition from density troughs in "shock-plus-D fronts."[9-12]

The Monte Carlo scheme.—The suprathermal electrons are particles with longitudinal (x-directed) and transverse velocity components. Following Jackson[13] the consequence of many small-angle Coulomb encounters is taken as a Gaussian distribution of new polar trajectory angles. The mean square angle of the Gaussian is $\langle\theta^2\rangle = 8\pi e^4 \times m^{-2}c^{-3}\Delta t Z n_i (Z+1)\ln\lambda$, in which c is the particle speed, n_i the background ion density, and in $Z+1$ the Z is for scattering from ions, while the $+1$ gives a term which approximates scattering from electrons. In each Δt random-number generators are called to pick a new θ for each particle and a new uniformly distributed azimuthal angle; then the particle speeds are reduced by Coulomb drag, $\Delta c = -4\pi e^4 n_c m^{-2} c^{-2}\Delta t \ln\lambda$, and projected as new velocity components. Here n_c is the thermal density; suprathermal electrons slowed to $c \leq 0$ are destroyed, appearing as increments Δn_c. Finally, the longitudinal velocity is changed by the electric field, and the particles are moved in x.

Particles are emitted from the first overdense cell in a 20° half-angle cone toward the laser to mock up resonant absorption. Typically, two particles are emitted each cycle in a drifting longitudinal Maxwellian characterized by $T_h \sim (I\lambda^2)^{1/3} \times T_c^{1/3}$. The particles have weights allowing a variable $T_c(t)$ and $I(t)$. Fluid moments n_h, u_h, T_h, etc., are attributed to an Eulerian mesh via particle-in-cell area weighting. The thermal density is decreased for each suprathermal particle created.

The thermal particles obey extended Braginskii[14] equations, i.e.,

$$\frac{\partial n_c}{\partial t} = -\frac{\partial}{\partial x}(n_c u_c) + \dot{n}_D - \dot{n}_L, \tag{1}$$

$$\frac{\partial (n_c u_c)}{\partial t} = -\frac{\partial}{\partial x}\left[n_c(u_c + T_c/m)\right] - \frac{e n_c E}{m} - \alpha(Z)\nu_c n_c u_c + \frac{3\beta(Z)\nu_c q_c}{5T_c} + \frac{\dot{\bar{P}}_D}{m} - \dot{n}_L u_c, \tag{2}$$

$$\frac{3}{2}\frac{\partial (n_c T_c)}{\partial t} = -\frac{3}{2}\frac{\partial}{\partial x}(n_c u_c T_c) - n_c T_c \frac{\partial u_c}{\partial x} + \alpha(Z)\nu_c m n_c u_c^2 - \frac{3\beta(Z)\nu_c}{5T_c} m u_c q_c + \dot{\bar{E}}_D - \tfrac{3}{2}\dot{n}_L T_c - \frac{\partial q_c}{\partial x}, \tag{3}$$

$$q_c = -\left(\frac{K}{\gamma(Z)}\frac{\partial T_c}{\partial x} + \frac{3\beta(Z)}{2\gamma(Z)} n_c u_c T_c\right)(1 + |F_L|/F_l)^{-1} \equiv q_d + q_u, \tag{4}$$

with $K \equiv 5n_c T_c/2m\nu_c$, $F_D \equiv -K/\gamma(Z)\partial T_c/dx$, and $F_l \equiv 0.6 n_c T_c^{3/2}$. The n_D and n_L terms are the rates of drag deposition and laser emission of suprathermals, while $\dot{\vec{P}}_L$ and $\dot{E}_L$ are the mean momentum and thermal energy transfer rate to the cold electrons by electron-electron collisions. Here α, β, and $\gamma(Z)$ are $O(1)$ functions[15] that can be related to Braginskii's tabulated coefficients, and $\nu_{c,h}$ are the cold- and hot-electron scattering rates off ions.[14] The thermal heat flux q_c, including its thermoelectric contribution q_u ($\sim n_c u_c \times T_c$), is limited to the classical value F_l. This form was chosen for the limiter upon noting that, in the next higher moment equation beyond (3) for $\partial q_c/\partial t$, the thermoelectric contribution passes to zero with ν_c. Equation (4) goes to Braginskii's result when $|F_D| \ll F_l$. The effects of ion-acoustic instability have been explored by adding to ν_c the additional rate[16] $\nu_{ia} = 3\times10^{-5}\omega_{p_c}|u_c|T_c/(v_c T_i) \times[m/m_i]^{1/4}$, where $v_c = (KT_c/m)^{1/2}$ and, typically, $T_i = 0.1$ keV. Equations (1)–(4) are advanced each time step by the donor-cell technique.[17] Below, $\Delta x = 1$ μm and $\Delta t = 2\times10^{-3}$ ps.

The electric field is obtained by updating

$$\partial E/\partial t = 4\pi\epsilon(n_h u_h + n_c u_c),$$
$$\epsilon = \frac{(\beta\Delta t)e}{(\omega_p^2\Delta t/n_t)[n_h/\nu_h' + n_c/\nu_c']} \leq e, \tag{5}$$

in which $\nu_{h,c}' = \nu_{h,c} + 1/\Delta t$, $n_t = n_h + n_c$, $\omega_p^2 = \omega_p^2(n_t)$ and, typically, $\beta\Delta t = 0.04$. In the corona the electric field grows on the plasma period time scale, which can be 10^2–10^3 times smaller than the Courant time step Δt. By using a charge ϵ lower than the physical value, we *dilate* the effective plasma period, such that $\omega_p^2|_{\rm eff} = 4\pi e\epsilon n_t/m \rightarrow 0.04/\Delta t^2$, or $\omega_p|_{\rm eff}\Delta t = 0.2$ as $\nu_{h,c} \rightarrow 0$, permitting a stable explicit calculation of E at Δt. Consequently, the Debye length for the hot electrons is stretched to $O(\Delta x)$, which is analogous to the stretching of classical shocks to the mesh dimension by the introduction of artifical viscosity. Experience with (5) shows that in a few times Δt it establishes the steady state $n_c u_c = -n_h u_h$, giving $E \simeq (\alpha - \frac{9}{10}\beta^2/\gamma)\nu_c n_h u_h$ in isothermal dense regions, and $E \simeq -(1/en_h)(\partial P_h/\partial x)$ in the corona. Details will be given elsewhere.[18]

Applications.—The scheme has been used to study transport in foillike geometries. Sample machine output is shown in Fig. 1. The foils are of SiO_2 ($\bar{Z} = 10$). The ions are *fixed*, i.e., at present we study the transport for only short intervals compared to the ion hydro times. The total electron charge density $n_t \simeq Zn_i$ rises from coronal values through critical (10^{21} cm^{-3}) to a plateau value[9-12,19] $\sim 1.3\times10^{21}$ cm^{-3} and then up to its solid density value $\sim 5\times10^{23}$ cm^{-3}. Laser light (1.06 μm) enters from the right.

It has been established[20] that return-current resistive electric fields can provide transient hot-e^- inhibition in cold targets. Our simulations show that at plateau densities in glass targets the inhibition sets in for *fixed* T_c below 100 eV. Runs with T_c as low as 1 eV show the hot electrons almost totally confined to a region near the critical surface, Figs. 1(a)–1(c). However, when T_c is allowed its *natural increase* from Joule heating, Coulomb drag, and conduction, the inhibition from resistivity "burns out" at a rate exceeding 30 μm/ps. Comparison of Figs. 1(a) and 1(e) shows much higher n_h values in the burned-out case at, say, 20 μm below the critical surface; the comparative phase plots (b) and (f) also demonstrate the reduced retention of the hot electrons with burnout. In fact, the hot-e^- results in Figs. 1(e) and 1(f) are essentially unaltered if we entirely suppress the electric field effects on hot electrons from $x < 36$ μm. The burnout time can be slightly longer at higher Z because of the larger ν_c, and considerably longer at higher density because of high specific heat. But even at $n_t \simeq 5\times10^{23}$ cm^{-3} in SiO_2 we find that the inhibition from E is at most only equivalent to that provided by classical hot-electron scattering.

Alternatively, the electric field from cold pressure gradients at large density jumps can overwhelm the resistive E for sufficiently large T_c, actually *enhancing* the suprathermal transport. In steady state, if we neglect source and thermoelectric terms, (2) becomes $E = -[\alpha(Z)\nu m_c j_c + \partial P_c/\partial x]/en_c$. From critical to solid density the potential energy change is $\Delta(e\varphi) \simeq T_c \ln(5\times10^{23}/10^{21}) = 6.2T_c$. So if $T_c = 2$ keV a hot electron gains 12 keV on running from critical to solid density. Figures 1(d) and 1(h) exhibit the effects of this acceleration mechanism.

Ion-acoustic turbulence is a suspected source of inhibition. The Lindman[16] effective ν_{ia} has been used in all our simulations. Generally, it is more than two orders of magnitude below ν_c. Multiplying ν_{ia} by 30 we found no effect on the hot electrons. But multiplication by 10^3 provided confinement comparable to that shown in Figs. 1(a)–1(c).

Cold convection and thermoelectric effects can inhibit the thermal transport. This has been generally overlooked. When we neglect sources and

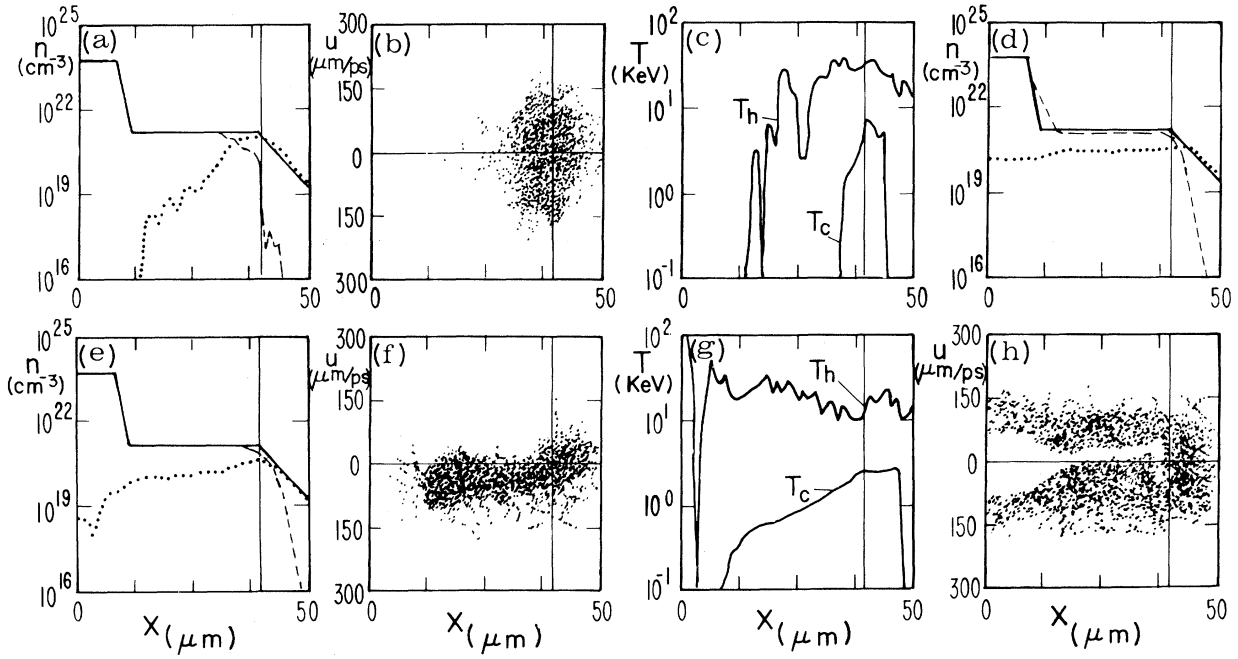

FIG. 1. Return-current resistive E calculations. Results after 1.8 ps of illumination at $I=5\times10^{15}$ W/cm^2 under the assumption of 35% absorption with 5% deposition into the thermal electrons as inverse bremsstrahlung. n_t, solid line; n_h, dotted line; n_c, dashed line. Initially $T_c=1$ eV. (a)–(c) T_c fixed for $x<36$ μm; (e)–(g) T_c may change. A vertical fiducial marks the critical surface. (d) and (h) show the transport-enhancing effect of the electric field containing high-density colds when $T_c=2$ keV initially; here the suprathermal scattering and drag have been suppressed. The hot electrons are accelerated as they drift into the high-density region, $x<12$ μm; this should enhance the preheat.

PdV work, (3) reduces to

$$\frac{3}{2}\frac{\partial}{\partial t}(n_c T_c) = -\frac{3}{2}\frac{\partial}{\partial x}(n_c u_c T_c) - \frac{\partial}{\partial x}(q_d + q_u).$$

The convection and thermoelectric terms move heat towards n_{crit} so that there can be net thermal inhibition and even *transport reversal* when $|\frac{3}{2}n_c u_c T_c + q_u| > |q_d|$. By quasineutrality $n_c u_c \simeq -n_c u_h$, and so this will occur in the presence of large suprathermal currents. This reversal effect is similar to Shkarofsky's recent bi-Maxwellian results,[8] but it occurs here at high relative drift speed between the components, and even in the absence of collisions.

The conditions for reversal are straightforward under flux limitation. We have $q_t \to 0.6 n_c v_c T_c = F_l$ and $q_u \to 0$, so that we need $|\frac{3}{2}n_c u_c T_c| > 0.6 n_c v_c T_c$ or $|u_c| = (n_h/n_c)|u_h| > 0.4\, v_c$. Note, for example, that for 20-keV suprathermals $u_h = 60$ μm/ps, while for 4-keV thermals $v_c = 27$ μm/ps. Thus, typically, reversed heat flow should occur for $u_c > 11$ μm/ps or $n_h/n_c > 0.18$. The conditions are less stringent if the diffusion is unlimited, i.e., $|q_d| \ll F_l$. The mechanism should be stronger under Nd than CO_2 illumination, with assumption of a plateau density n_t independent of wavelength[20] as a result of the ponderomotive force, since $I \sim n_h u_h T_h$ and, generally, $T_h{}^{CO_2}/T_h{}^{Nd} \sim 4$, so that $n_h u_h$ is roughly four times stronger for Nd, yielding more inhibition by convection.

Figures 2(a) and 2(b) display the effects of the convective term. We find that, in practice, significant inhibition is difficult to achieve with this mechanism. First, this is true because *Joule heating* tends to mask the convective effects. So going to higher Z to reduce q_d may result in increased heating and an apparent reduction in the inhibition. Second, in general, the necessary high n_h/n_t ratios are unlikely since, for example, at high intensities[21] $n_h \sim I^{1/2}$, while $n_t \sim I$.

As a possible resolution of the difficulties we have found that assumed *density troughs* can markedly intensify the convection inhibition. Troughs have been calculated[9-11] and seen in experiment,[12] but their depth remains uncertain. Troughs decrease the maximum q_d and increase n_h/n_t. Figures 2(c) and 2(d) show T_c "bottled up" behind a dip to $0.4\, n_{\text{crit}}$. More inhibition of the

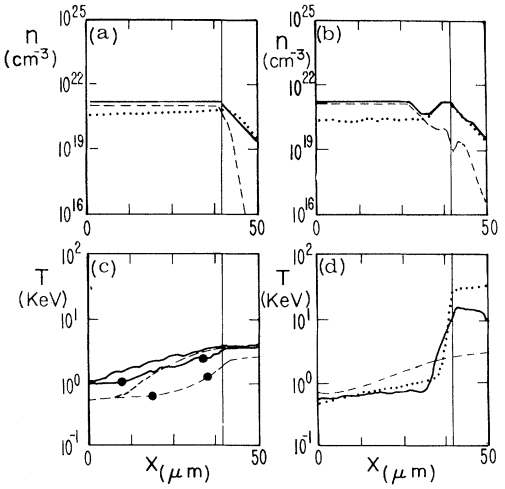

FIG. 2. Convective and trough inhibition results following 4 ps of the Fig. 1 illumination; left boundary a mirror. (a),(b) Typical density profiles with and without a trough; n_t, solid line; n_h, dotted line; n_c, dashed line. (c) No-trough T_c profile with Joule heating "on" (solid line), and "off" (dashed line); also with the convective term in (3) "on" (filled circles) and "off". Clearly the convective effects are stronger in the absence of Joule heating. (d) T_c profiles with the trough (solid line), and without it under classical limitation (dashed line), and under $\frac{1}{20}$ classical with the convective term "off" (dotted line). T_c with the trough is very similar to that with the limiter.

cold transport is achieved than with $\frac{1}{20}$ of the classical flux limiter in the absence of a trough. With a dip to $0.1n_{crit}$ the troughs are vacuum insulators,[22] even stopping the hot electrons, as in Figs. 1(a)–1(c). Thus, strong inhibition in "isotropic" experiments may be a signature for deep troughs in the target-density profiles.

The author is grateful to R. Morse, C. Nielsen, K. Lee, and W. Gula for early help with the collisional modeling, to D. Kershaw and A. Petschek for suggestions improving the dilation technique, and to P. Roberts, C. Cranfill, D. Forslund, and H. Brysk for helpful discussions. This work was performed under the auspices of the United States Department of Energy.

[1]G. S. Fraley and R. J. Mason, Phys. Rev. Lett. 35, 520 (1975).
[2]R. C. Malone, R. L. McCrory, and R. L. Morse, Phys. Rev. Lett. 34, 721 (1975).
[3]W. L. Kruer, to be published.
[4]G. Zimmerman, University of California Radiation Laboratory Report No. UCRL-74811, 1973 (unpublished).
[5]J. Delettrez and E. B. Goldman, University of Rochester Laboratory for Laser Energetics Report No. 36, 1976 (unpublished).
[6]D. Shvarts, C. Jablon, I. B. Bernstein, J. Virmont, and P. Mora, to be published.
[7]R. J. Mason, Phys. Rev. Lett. 42, 239 (1979).
[8]I. P. Shkarofsky, Phys. Rev. Lett. 42, 1342 (1979).
[9]C. E. Max and C. F. McKee, Phys. Rev. Lett. 39, 1336 (1977).
[10]K. A. Brueckner and R. J. Janda, Nucl. Fus. 17, 452 (1977).
[11]J. Virmont, R. Pellat, and A. Mora, Phys. Fluids 21, 567 (1978).
[12]R. Fedosejevs, M. D. J. Burgess, G. D. Enright, and M. C. Richardson, to be published.
[13]J. D. Jackson, *Classical Electrodynamics* (Wiley, New York, 1962), p. 457.
[14]S. I. Braginskii, Rev. Plasma Phys. 1, 205 (1965).
[15]C. Cranfill, to be published.
[16]E. Lindman, J. Phys. (Paris), Colloq. 38, C6-9 (1977).
[17]R. A. Gentry, R. E. Martin, and B. J. Daly, J. Comp. Phys. 1, 87 (1966).
[18]R. J. Mason, to be published.
[19]K. Lee, D. W. Forslund, J. M. Kindel, and E. L. Lindman, Phys. Fluids 20, 51 (1977).
[20]D. W. Forslund, J. M. Kindel, and K. Lee, Phys. Rev. Lett. 39, 284 (1977).
[21]E. J. Valeo and I. B. Bernstein, Phys. Fluids 19, 1348 (1976).
[22]K. Lee, D. W. Forslund, J. M. Kindel, and E. L. Lindman, to be published.